HHS Public Access

Author manuscript

Kidney Int. Author manuscript; available in PMC 2016 March 01.

Published in final edited form as:

Kidney Int. 2015 September ; 88(3): 490–502. doi:10.1038/ki.2015.73.

Migration of smooth muscle cells from the arterial anastomosis of arteriovenous fistulas requires Notch activation to form neointima

Ming Liang[1,2], **Yun Wang**[2], **Anlin Liang**[2], **William E. Mitch**[2], **Prabir Roy-Chaudhury**[3], **Guofeng Han**[4,2], and **Jizhong Cheng**[2,*]

[1]Department of Nephrology, Guangzhou First People's Hospital, Guangzhou Medical University, China

[2]Division of Nephrology, Department of Medicine, Baylor College of Medicine, Houston, Texas, United States

[3]Department of Surgery, Pathology and Radiology and Division of Nephrology, Department of Medicine, University of Cincinnati and Cincinnati VAMC, Cincinnati, Ohio, USA

[4]The 455th Hospital, Shanghai, China

Abstract

A major factor contributing to failure of arteriovenous fistulas (AVFs) is migration of smooth muscle cells into the forming neointima. To identify the source of smooth muscle cells in neointima, we created end-to-end AVFs by anastomosing the common carotid artery to the jugular vein and studied neural crest-derived smooth muscle cells from the carotid artery which are Wnt1-positive during development. In Wnt1-cre-GFP mice, smooth muscle cells in the carotid artery but not the jugular vein are labeled with GFP. About half of the cells were GFP-positive in the neointima indicating their migration from the carotid artery to the jugular vein in AVFs created in these mice. Since fibroblast-specific protein-1 (FSP-1) regulates smooth muscle cell migration, we examined FSP-1 in failed AVFs and polytetrafluoroethylene (PTFE) grafts from patients with ESRD or from AVFs in mice with chronic kidney disease. In smooth muscle cells of AVFs or PTFE grafts, FSP-1 and activation of Notch1 are present. In smooth muscle cells, Notch1 increased RBP-Jκ transcription factor activity and RBP-Jκ stimulated FSP-1 expression. Conditional knockout of RBP-Jκ in smooth muscle cells or general knockout of FSP-1, suppressed neointima formation in AVFs in mice. Thus, the artery of AVFs is the major source of smooth muscle cells during neointima formation. Knockout of RBP-Jκ or FSP-1 ameliorates neointima formation and might improve AVF patency during long-term follow up.

*Corresponding Author: Dr. Jizhong Cheng, Department of Medicine, Baylor College of Medicine, Houston, TX 77030, Tel: 713-798-2698, Fax: 713-798-5010, jizhongc@bcm.edu.

Disclosure

None

Keywords

arteriovenous fistula; chronic kidney disease; vascular smooth muscle cell; Notch; fibroblast specific protein 1; neointima formation

Introduction

The success of hemodialysis treatment depends on reliable functioning of an arteriovenous fistula (AVF) or polytetrafluoroethylene (PTFE) graft. But, in the 2 years following creation of the AVF or PTFE graft, nearly 50% fail, generally due to the accumulation of vascular smooth muscle cells (SMCs) in the neointima.[1–3] This problem is costly as loss of AVFs amounts to >$1 billion dollars per year for surgical and radiological interventions.

Multiple types of cells have been implicated in the formation of a neointima, including fibrocytes and bone marrow-derived, circulating progenitor cells, and/or endothelial-mesenchymal transition cells.[4–6] Besides circulating cells, neointima could be formed from local events and local cells, including resident SMCs, or adventitial cells and smooth muscle progenitor cells. The latter cells can transform into SMCs and participate in formation of the neointima.[7–10] To identify the origin of cells contributing to SMCs in the neointima, we used Wnt1-Cre transgenic mice to label and track neointima SMCs arising from the cardiac outflow tract.[11] Our strategy was based on the finding that during cardiac development, neural crest cells contribute to the smooth muscle layer of the cardiac outflow tract which includes the common carotid artery. Since SMCs arising from vessels that are outside of the neural crest (e.g., the jugular vein) are not labeled.[12–14] This strategy allowed us to examine whether SMCs from the arterial anastomoses contribute to the forming neointima.

What could regulate SMC functions in AVFs? Several important SMC growth-regulatory pathways and molecules can modulate neointima formation. These factors include transforming growth factor-β (TGF-β1) and Notch as well as Fibroblast Specific Protein 1 (FSP-1).[15, 16] FSP-1 is stimulated by growth factors which influence SMC migration and proliferation.[17] In fact, bone marrow-derived FSP-1 positive cells were shown to stimulate neointima formation in a mouse model of a vein graft.[18] Others have demonstrated that activation of Notch can promote the vascular remodeling that follows vessel injury.[15, 16]

Recently, we developed a mouse model of an AVF model and used it to show that chronic kidney disease (CKD) accelerates neointima formation.[16] There was evidence for endothelial damage in the AVFs of mice with CKD.[19] Specifically, the endothelium of the AVF became leaky, leading to the infiltration of inflammatory cells causing activation of SMCs. Our goals in the present experiments were to identify the origin of SMCs and how their migration is regulated during neointima formation. Our results identify potential targets that might prevent neointima formation in AVFs, the "*Achilles* heel" of the hemodialysis patient.

Results

SMCs from the arterial anastomosis contribute to neointima formation

We used a Wnt1-Cre reporter mouse strain in which SMCs from the artery are specifically labeled while venous SMCs were not labeled. Wnt1-Cre transgenic mice with dual-fluorescent, RFP-Stop$^{flox/flox}$-GFP/Wnt1-Cre^{+} mice (Supplemental figure 1), were studied to determine if SMCs in the neointima are derived from the artery of an AVF. This identification was possible because SMCs of the cardiac outflow tract express GFP in Wnt1-Cre^{+} reporter mice, but other, non-neuron, crest-derived cells (including SMCs of the vein) are positive for RFP. While SMCs from the common carotid artery in RFP-Stop$^{flox/flox}$-GFP/Wnt1-Cre^{+} mice were GFP^{+}, endothelial cells were RFP^{+} (Fig. 1A), GFP and RFP signals were not co-localized. There also was no non-specific staining of elastin (Fig. 1A). Note that endothelial cells or SMCs arising from the jugular vein were not GFP-positive signals (Fig. 1A). Next, we examined whether GFP^{+}-SMCs were present in AVFs created in the RFP-Stop$^{flox/flox}$-GFP/Wnt1-Cre^{+} mice. GFP positive cells were observed in frozen sections of the neointima at the venous side near the anastomosis (Fig. 1B). Co-staining with a SMC marker showed that around 50% of neointima cells in the AVF were GFP-positive and most expressed SMA-α. There were some GFP-negative SMCs in the neointima of the AVFs (Fig. 1C). Our results indicate that SMCs from anastomosed artery contribute to as much as 50% of SMCs in the neointima.

As expected, Wnt1 was expressed in the vagus nerve (Fig. 1D) but was not detected in neointima cells of AVFs (Fig. 1E). These results indicate that: 1) Wnt1 is expressed and will activate Cre in the vagus nerve leading to GFP expression; and 2) GFP-positive SMCs present in the forming neointima originated from neural crest-derived SMCs because they were Wnt1-negative but GFP-positive. The results raise the question, what stimulates arterial SMCs to migrate into the forming neointima?

CKD stimulates FSP-1 expression and Notch activation in SMCs of the neointima

There were significantly increased mRNA levels of FSP-1 in the AVFs created in mice with CKD (Fig. 2A). In fact, there was increased expression of the FSP-1 protein in cells of the neointima in AVFs created in mice with CKD vs. results in control mice (Fig. 2B & C). Notably, FSP-1-positive cells in the neointima also stained positive for SMA-α (Fig. 2D). We characterized neointima cells by staining for the SMC terminal differentiation marker (smooth muscle myosin heavy chain, SMMHC). These neointima cells co-stained positively for SMMHC and SMA-α, indicating that SMCs are present in the neointima (Fig. 2E). Immunostaining for vimentin was detected in the adventitia and was slightly stained in the neointima (Fig. 2F), Notably, these vimentin-positive cells co-stained positively with FSP-1 (Fig. 2G). We conclude that SMCs are the major cellular contributor to neointima formation because they express the terminal differentiation marker of SMCs, SMMHC.

Since Notch activation and Notch/RBP-Jκ signaling have been linked to worsening of vascular remodeling in arterial injury models,[20, 21] we examined how CKD affects Notch and its signaling pathway. CKD increased the expression of Notch receptors and their target genes, Hes1 and Hey1 in AVFs (Fig. 2H). CKD also was associated with activation of

Notch 1 (N1ICD) which was present in nuclei of neointima cells co-expressing FSP-1 (Fig. 2I). Thus, FSP-1 expression could be regulated by Notch signaling pathway.

Notch regulates FSP-1 transcription

In AVFs created in CKD mice, Notch activation was increased compared to results in AVFs placed in control mice. A potential mediator is TGF-β1 because it can stimulate Notch activation[22, 23] In fact, we found that adding TGF-β1 to SMCs induced the cells to express both the Notch ligand, Jagged1 and FSP-1 in a time-dependent fashion (Fig. 3A). Since we found that the TGF-β1-induced FSP-1 expression is suppressed by pretreatment with the Notch inhibitor, DAPT (Fig. 3B), our results suggest that CKD induces FSP-1 expression via a TGF-β1 to Notch pathway.

We examined the FSP-1 promoter and found potential binding sites of RBP-Jκ upstream of the transcription start site (TSS) (Fig. 3C). To determine if RBP-Jκ targeting sites in FSP-1 promoter can activate the transcription of FSP-1, we created luciferase-reporter constructs of different fragments of the FSP-1 promoter (left panel of Fig. 3D). In the absence of RBP-Jκ sequences, there was no increase in luciferase activity in response to TGF-β1 (Fig. 3D, right panel). Moreover, DAPT, the Notch inhibitor, suppressed TGF-β1-induced FSP-1 promoter activity by ~50% in cultured SMCs (Fig. 3E). In SMCs, KO of RBP-Jκ suppressed TGF-β1-induced FSP-1 promoter activities by ~40% vs. results in wild type SMCs (Fig. 3F). Together, these results indicate that Notch activation stimulates FSP-1 transcription.

TGF-β1-stimulated DNA binding activity is regulated by Notch signaling

We designed 8 pairs of primers (P1 to P8) to amplify the DNA fragments that contain the potential RBP-Jκ binding elements present in the FSP-1 promoter (Supplemental Table 1). In SMCs treated with TGF-β1, a ChIP assay revealed that TGF-β1 induces N1ICD-dependent, DNA binding activity. DNA binding increased with primer sets 2, 5, and 6 (primer 6 generated the strongest activity (Fig. 4A)). Pretreatment of SMCs with DAPT or expression of a soluble Jagged1 protein (inhibiting Notch signal) blocked TGF-β1-induced NICD binding activity to the primer 6 sequence (Fig. 4B &D). In contrast, when full length of Jagged1 was expressed, there was enhanced N1ICD binding activity in the same region of the FSP-1 promoter. This response was blocked by Notch inhibitors (Fig. 4C & E).

To identify the specificity of RBP-Jκ binding to elements of the FSP-1 promoter, we designed a probe based on primer 6 and performed an EMSA analysis (probe sequence; Supplemental Table 2). At 2 hours after treating SMCs with TGF-β1, there was increased protein-DNA binding activity. Pre-exposure to the Notch inhibitor, DAPT, blocked these TGF-β1-induced responses (Fig. 4F). Overexpression of full length Jagged1, markedly stimulated DNA binding activity in SMCs. DAPT suppressed this protein-DNA binding activity (Fig. 4G). A super-shift analysis indicates that Jagged1 binding activity can be prevented by antibodies against N1ICD or RBP-Jκ (Fig. 4H). The probe from primer set 4 (See supplemental Table 2) was also subjected to EMSA analysis. In this case, addition of TGF-β1 or overexpression of full length Jagged1 did not cause a DNA shift (Supplemental figurer 2). These results demonstrate that binding of the Notch/RBP-Jκ pathway to a specific sequence of the FSP-1 promoter regulates FSP-1 transcription.

RBP-Jκ KO in SMC suppresses FSP-1 expression and neointima formation

To determine whether RBP-Jκ can regulate SMC migration, SMCs from control and RBP-Jκ KO were studied. The TGF-β1-stimulated SMC outgrowth was suppressed in SMC with RBP-Jκ KO (Fig. 5A). Next, we created AVFs in RBP-J$\kappa^{flox/flox}$/SMMHC-CreER^{T2+} mice (RBP-Jκ KO mice) so that RBP-Jκ could be specifically knocked out in SMCs upon induction with tamoxifen. In AVFs created in RBP-Jκ KO mice, RBP-Jκ expression was absent in neointima cells but was present in endothelial or adventitial cells (Fig. 5B). The expression of FSP-1 in the neointima was significantly decreased in AVFs from RBP-Jκ KO mice (Fig. 5B). In CKD mice, the accumulation of SMC and extracellular matrix was significantly decreased in the neointima RBP-JK KO mice (Fig. 5C). This response resulted in a higher lumen to neointima ratio when compared to wild type mice (Fig. 5D), which might result in increased patency of the AVF during long-term follow up.

Blocking FSP-1 inhibits CKD-stimulated neointima formation in AVFs

In an *ex vivo* outgrowth experiment, we observed that FSP-1 KO suppressed the Jagged1-induced outgrowth of SMCs (Fig. 6A). Overexpression of full length Jagged1 induced FSP-1 expression in SMCs (Fig. 6B). Outgrowth of SMCs isolated from AVFs of FSP-1 KO mice exhibited fewer cells vs. results from SMCs obtained from AVFs placed in control mice (Fig. 6C). The defect in SMCs outgrowth was eliminated when FSP-1 was overexpressed (Fig. 6C & D). Interestingly, the areas of neointima in AVFs of FSP-1 KO mice were significantly reduced while the ratio of lumen to neointima areas was increased (Fig. 6E).

In human AVFs, neointima cells express activated Notch and FSP-1

To examine if our results are relevant to patients with ESRD, we examined failed AVFs from 5 ESRD patients. The lumens of failed AVFs were almost occluded by the neointima (Fig. 7A). Cells in the smooth muscle layer of the vein and neointima but not in the adventitia were SMA-α^+ (Fig. 7A). In fact, >95% of cells in the neointima positively immunostained for FSP-1 and the cell proliferation marker, PCNA (Fig. 7B, red arrow). In contrast, SMCs present in the media of veins of the AVF in did not express either FSP-1 or PCNA (Fig. 7B, green arrow). In the neointima of failed AVFs, SMA-α and FSP-1 were co-expressed in SMCs of the neointima but not in the media of veins of the AVF (Fig. 7C).

In failed AVFs from ESRD patients, activated Notch 1 (N1ICD) was present in nuclei of neointima cells (Fig. 7D). These cells also were FSP-1 positive (Fig. 7E). There were no N1ICD-positive cells in the media of veins of the AVF. Thus, SMA-α positive neointimal cells in failed AVFs of ESRD patients exhibit similar properties to those in the mouse model of CKD.

Stenosis also occurs in failed PTFE grafts,[24]. H&E and Trichrome staining of PTFE grafts reveal accumulation of collagen and fibrin in the neointima (Fig. 7F) with cells that were SMA-α positive, and costained with FSP-1 (Fig. 7G). The pathologic in failed AVFs and PTFE grafts from ESRD patients were similar. There was more extracellular matrix deposition and fewer SMCs in the failed PTFE grafts. There also was evidence of N1ICD

expression in neointima cells with FSP-1 co-staining in PTFE grafts (Fig. 7H), consistent with activated Notch signaling in neointima cells in both AVFs and PTFE grafts.

Discussion

A functioning arteriovenous fistula (AVF) is critical for the success of hemodialysis but as many as 50% of AVFs fail within two years, mainly due to neointima formation. In a mouse model of the AVF, we investigated the relationships between CKD and failure of the AVF and discovered that SMCs migrating from the arterial anastomosis of an AVF are a major source of cells from the neointima. Secondly, we uncovered that FSP-1 is a key mediator that promotes SMC migration from the AVF artery principally to the vein. In failed AVFs from ESRD patients or in a mouse model of CKD there was increased expression of FSP-1 in SMCs. Thirdly, we found that activated Notch1 stimulates the transcription factor, RBP-Jκ, to initiate transcription of FSP-1 providing a stimulus for SMCs to migrate into the neointima. Indeed, we found that targeted disruption of FSP-1 expression or KO of RBP-Jκ in SMCs suppresses neointima formation and delays failure of the AVF. We conclude that targeting RBP-Jκ/FSP-1 signaling could interfere with migration of SMCs into the forming neointima, slowing the loss of AVF patency.

In the AVF, neointima formation from SMC accumulation and extracellular matrix deposition is a hallmark of AVF failure and therefore, understanding the origin of SMCs in the forming neointima is critical for designing therapeutic strategies to prevent AVF failure.[25, 26] Recently, Owens et al. concluded that neointima cells in AVFs could arise from an arterial anastomosis, from the bone marrow, from the adventitia or from circulating cells.[8] Other investigators have concentrated on identifying a single source of SMCs in the neointima. For example, Hagensen, et al., studied a model of arterial injury and reported that SMCs from the anastomosed or “neighboring” artery is the only source of SMCs in the neointima.[27] In contrast, Tanaka, et al. reported that SMCs from the bone marrow are a major source of SMCs in neointima formed in response to arterial injury.[28] This is controversial, however, as other investigators conclude that bone marrow cells do not transdifferentiate into SMCs [29, 30] Besides these experiments, it has been suggested that SMCs from the vein grafted into the aorta can play an essential role in the formation of neointima in rat AVFs.[31] Finally, myofibroblasts in the adventitia have been proposed as precursors of SMCs found in growing neointima.[10, 32] We used a different strategy based on the finding that cells arising from the neural crest can be genetically labeled in Wnt1-Cre reporter mice. Our results show that SMCs from the anastomosed artery migrate into the neointima to form as many as 50% of the cells in the neointima of the AVF.

Previous reports conclude that the accumulation of neointima cells results from migration and proliferation of adventitial myofibroblasts, characterized by positive staining of SMA-α in the cells.[33] The difficulty in interpreting these reports is that SMA-α is expressed both in SMCs and in myofibroblasts. Specifically, to identify SMCs, other markers are needed: we found that SMA-α-positive neointima cells co-express the SMC terminal differentiation marker, SMMHC. Consequently, neointima cells are principally SMCs rather than myofibroblasts.

Vimentin has been used as a marker for myofibroblasts in the kidney, in human PTFE vascular grafts and in AVFs.[24, 34] It is the most ubiquitous intermediate filament protein and is expressed in a variety of cells, including myofibroblasts,[35] endothelial cell,[36, 37] and hematopoietic cells.[38] We have found that vimentin is not only expressed in the adventitial cells, including myofibroblasts but is also expressed in $SMMHC^+$ SMCs in the neointima of AVFs (Fig. 2). For these reasons, markers other than vimentin should be used to differentiate myofibroblasts or fibroblasts from SMCs in AVFs. Similar results are reported in models of vascular injury, indicating that vimentin is expressed in SMCs as well as myofibroblasts.[39] Thus, the neointima cells we found to be stained positively with vimentin are most likely to be SMCs.

Regarding stimuli for migration of SMCs, we studied FSP-1, (also known as metastasin) as it is expressed in metastatic cells and will promote cell migration following direct binding to myosin IIA.[40] It also can regulate the cellular motility of SMCs in part by suppressing tissue inhibitors of metalloproteinases (TIMP).[41, 42] FSP-1 can play a role in vascular remodeling. For example, Brisset et al. studied SMCs isolated from clogged human coronary arteries and found that the SMCs that expressed FSP-1, exhibited a higher potential for migration and proliferation.[43] In ESRD patients, we found that FSP-1 expression is significantly increased only in neointima cells of failed AVFs. Experimentally, we found that FSP-1 KO inhibits SMC migration and protects against uremia stimulated neointima formation (Fig. 7). These results suggest that targeting FSP-1 could suppress neointima formation.

Notch signaling can regulate vascular remodeling. For example, in models of vascular injury, inhibition of the Notch ligand, Jagged1, or knockdown of Notch, ameliorates neointima formation.[20, 44] We have extended this finding and showed that activated Notch1 is also present in SMCs of the neointima in AVFs. In SMCs, activated Notch transduces signals via RBP-Jκ, a transcription factor that regulates FSP-1 expression. We found that blocking Notch with an inhibitor of or KO of RBP-Jκ partially blocks FSP-1 expression, suggesting other signaling pathways can manipulate FSP-1 expression. For example, there are growth factors that induce FSP-1 expression through activating the transcription factor NF-kB or NFAT.[45, 46] Serotonin also can stimulate the release of FSP-1 through G-protein coupled receptor in SMCs.[47] Thus, multiple signaling pathways regulate FSP-1 expression.

In failed human PTFE grafts, there is evidence of Notch activation and FSP-1 expression similar to characteristics of SMCs that are present in AVFs of ESRD patients (Fig. 7). This suggests that the same signaling pathway mediates SMC migration and accumulation in PTFE grafts and in failed AVFs from ESRD patients. We examined a relatively small number of failed PTFE grafts and found forming neointima in venous anastomosis of the PTFE grafts. Obviously, we cannot analyze the origin of SMCs in human samples as we have done in the mouse model of the AVFs. Still it is tempting to speculate that there are similarities in neointima formation in failed human PTFE grafts and the mouse AVFs as both has accumulation of SMCs in the venous anastomosis. Secondly, we find only 50% of SMCs in the neointima in AVFs arise from the artery. Thus, cells besides those from the bone marrow, the adventitia or the vein could give rise to SMCs in the forming neointima in the venous side of PTFE grafts.

The mouse AVF model we developed is an end-to-end AVF. We recognize that this model differs from AVFs placed in ESRD patients, as they are mainly end-to-side anastomoses. Besides our model, a recent development is the end-to-side anastomosis in mice.[48] The responses found in this model include cellular events, morphology, and pathological changes that are similar to those we find in the AVF model we studied.[16] Both mouse models develop an initial endothelial denudation followed by infiltration of inflammatory cells in the AVFs with accumulation of SMCs in the neointima. However, differences in the surgical technique could affect blood flow and hemodynamics resulting in varied responses in the AVF. In the AVF model we studied, the similarities of responses in failed AVFs in ESRD patients indicate that the mouse model of an AVF we studied can be used to study mechanisms of AVF failure.

Our results provide insights into the mechanism yielding neointima formation in AVFs. If additional characteristics are found to be similar in AVFs in ESRD patients and in the mouse model, a new treatment strategy could be developed to suppress the migration of SMCs into the forming neointima.

Concise Methods

Mice with CKD

All studies were approved by the Institutional Animal Care and Use Committee of Baylor College of Medicine in accordance with NIH guidelines. Male wild type or FSP-1 KO transgenic mice or LacZ-Stop^{flox}, Wnt1-Cre, and RFP-Stop$^{flox/flox}$-GFP mice were from Jackson Laboratory (Bar Harbor, Maine). They were kept in a 12-h light/12-h dark cycle. RBP-Jκ-floxed mice were kindly provided by Dr. K. Susztak (Albert Einstein College of Medicine, NY). To generate RFP-Stop$^{flox/flox}$-GFP/Wnt1-Cre^{+} mice, the RFP gene allele was deleted by Cre recombination; GFP begins to be expressed in SMCs of the cardiac out flow tract. SMMHC-CreER^{T2} transgenic mice were obtained from Dr. S. Offermanns (Max-Planck-Institute for Heart and Lung Research). The RBP-Jκ$^{flox/flox}$/SMMHC-CreER^{T2} transgenic mice were created, and RBP-Jκ deletion was induced by Tamoxifen (2 mg/mouse/day I.P. for 5 days).

CKD in anesthetized mice (ketamine, 125 mg/kg BW and xylazine, 6.4 mg/kg BW) was induced by subtotal nephrectomy as described.[49, 50] Briefly, mice matched for body weight underwent two-step subtotal nephrectomy: first, ~3/4 of the left kidney was removed and post operatively, the mice were given 2 doses of buprenorphine (0.1–2.5 mg/kg BW by subcutaneous injection) after surgery and 12 hours later. To reduce mortality and limit kidney hypertrophy, mice were fed 6% Protein Rodent Diet Chow (Harlan Teklad, Madison, WI, USA) *ad libitum*. One week later, the right kidney was removed from anesthetized mice. After one week of recovery, mice with CKD were fed 40% protein chow and compared to sham-operated control mice. Levels of BUN and serum creatinine were measured. After 2–3 weeks, AVFs were created in control, and CKD mice while other control and CKD mice underwent sham surgery.

Human AVF, PTFE grafts and Mouse AVF Model

We studied samples of AVFs from five ESRD patients ranging in age from 58 to 77 years. After obtaining approval of the Baylor Institutional Review Board, samples of failed AVFs were collected at surgery. In addition, we studied 7 PTFE samples from ESRD patients treated at the University of Cincinati, Cincinnati, Ohio, USA and the 544th Hospital, Shanghai, China. In these samples, we evaluated the morphology and staining of cell markers at the anastomosis of graft to the vein. AVFs in mice were created as described.[16] Briefly, the right internal jugular vein was isolated and its distal end ligated while the proximal common carotid artery was ligated below its bifurcation. An end-to-end anastomosis was created using 11-0 nylon suture with an interrupted stitch. After unclamping, patency was confirmed visually. The mice were kept warm after surgery and the analgesic (buprenorphine) was given twice at 12 hours apart. At 2 and 4 weeks after surgery, anesthetized mice were euthanized by perfusing the left ventricle with PBS and 10% formalin for 10 min. AVFs were identified and sections were obtained from 0.2 to 1 mm from the venous anastomosis. AVF's from 5 hemodialysis patients were collected and evaluated as described.[19]

Reagents and virus

Penicillin, streptomycin, DMEM, and FBS and the fluorescent-700 or -800 secondary antibodies were obtained from Invitrogen (Invitrogen Life Technologies; Carlsbad, CA). The γ-secretase Notch inhibitor, DAPT, was from Calbiochem (San Diego, CA) while human TGF-β1 was obtained from R&D (Minneapolis, MN). Antibodies against Notch 1-ICD, Wnt1, and SMA-α (rabbit) antibody were from Abcam (Cambridge, MA), while antibodies against smooth muscle myosin heavy chain (SMMHC), SMA-α-FITC, and β-actin were from Sigma-Aldrich (Louis, MO). The FSP1 antibody was from DAKO (Carpentaria, MA). Antibodies against PCNA (rabbit), Jagged1, Hes1, TGF-β1 and β-actin antibodies were from Santa Cruz Biotechnology (Santa Cruz, CA). The anti-GFP monoclonal antibodies and polyclonal antibodies were obtained from Invitrogen (Carlsbad, CA) and Abcam (Cambridge, MA), respectively. Antibody against vimentin was from Genescript USA Inc (Piscataway, NJ). The full-length, Jagged-1 recombinant adenovirus was kindly provided by Dr. M.J. Post (Maastricht University, Netherlands). The FSP-1 overexpressing adenovirus and FSP1 shRNA lentivirus were used as described.[18] The FSP-1 expression adenovirus was kindly provided by Dr. TC He (University of Chicago).

Luciferase plasmid construction

Up to 2.9 kb upstream from the transcription start site, the FSP-1 promoter contains 12 RBP-Jκ potential binding sites (Fig. 6). To determine FSP-1 promoter activity, the full length of FSP-1 promoter and selected fragments in the promoter were cloned into a luciferase vector. The Bgl I restriction enzyme recognition sites (underlined) were added at 5′-ends of upstream and downstream primers (5′-GGCCTAACTGGCCATCGTGTGCACCTTCCAGGAGTAT-3′; 5′-GGCCGCCGAGGCCAAGTGCTCTATCCCAGCCAACTCT-3′; Bgl I restriction site was underlined) for full length of FSP-1 promoter pFSP-1A. Fragments containing different parts of the FSP-1 promoter were amplified by using primers (5′-

GGCCTAACTGGCCTACTACTGGAGGTAGGAGGCTTA-3′ for luciferase vector pFSP-1B; 5′-GGCCTAACTGGCCATGAGCGTATGGGTTG-3′ for contruct pFSP-1C; and 5′-GGCCTAACTGGCCGAGTAAGCTGATGG-3′ for pFSP-1D); the PCR fragments were cloned into a firefly luciferase, pGL4.1-Luc, vector (Promega, Madison, WI).

Transient Transfection and Luciferase Assay

Using Lipofectamine 2000 (Invitrogen, Carlsbad, CA), mouse SMCs were transfected with FSP-1 luciferase plasmids. Transfected cells were incubated in serum-free media for 24 hours before being treated with TGF-β1 for 24 hours. pRL-TK was co-transfected and the level of firefly luciferase activity was normalized to Renilla luciferase activity measured by the dual luciferase system (Promega, Madison, WI).

Chromatin Immunoprecipitation Assay (ChIP)

Chromosomal DNA (QiGene DNA Purification kit) was isolated from normal SMCs or from SMCs treated with TGF-β1 or Notch ligands. The DNA was immunoprecipitated with the anti-N1ICD antibody and ChIP analysis was performed according to the manufacture's protocol (Upstate Biotechnology, Lake Placid, NY) with some modification.[51] A total of 8 pairs of primers (Supplemental Table 1) were used to amplify DNA fragments that overlap RBP-Jκ binding sites in FSP-1 promoter. DNA samples before immunoprecipitation were used as a template for input control.

Electrophoretic Mobility Shift Assay (EMSA)

Based on results of the ChIP assay, an oligonucleotide containing RBP-Jκ binding sites was selected for further characterization with EMSA analysis. Double-stranded oligonucleotides were synthesized (5′-CTTGGTGGCAAGCACCTCTACCCACTGAG-3′; and 5′-CTCAGTGGGTAGAGGTGC TTGCCACCAAG-3′) (potential RBP-Jκ sites were underlined); the forward probe was labeled with the fluorescent dye IRdye 800 (IDT, Coralville, Iowa) at its 5′ end and purified by HPLC. It was used to measure the DNA-binding activity of RBP-Jκ in the EMSA assay. Extracts from nuclei of VSMCs were prepared as described.[52]

Wound healing assay

SMCs were seeded in 6 well plates in DMEM containing 2 mM glutamine, 100 U/ml penicillin, 0.1 mg/ml streptomycin and 10% fetal calf serum. Following TGF-β1 treatment (2 ng/ml) or infection with Jagged1 or AdFSP-1, SMC were wounded with a 200-μl tip, washed with PBS and incubated at 37°C in DMEM media. At different times, pictures were taken to record the SMC migration toward the open area.

Ex vivo culture of mouse common carotid arteries

Mouse common carotid arteries were collected from WT, FSP-1 KO, or RBP-Jκ KO mice and assayed.[53] The arteries were opened longitudinally and cut transversely into small (0.2 cm) segments. These segments were seeded onto 12-well plates with luminal surface facing down and cultured individually in the DMEM media. AdFSP-1 or AdJagged1 were added

and the treatment and culture media were replaced every other day. Outgrowth of the SMCs was recorded.

Immunohistochemistry

Sections were blocked with 10% goat serum (Vector Laboratories, Burlingame, CA) for 30 min before being incubated with primary antibodies (NICD,1:500; RBP-Jκ,1:500; FSP-1, 1:1000; α-SMA, 1:2000). Sections were washed in 0.5% Tween 20 in PBS (PBST) and incubated at RT with a biotinylated secondary antibody (Vector lab). After PBST washes, tissue sections were incubated with an *Elite*® ABC reagent (Vector Laboratories) followed by instructions as described in a peroxidase substrate kit (Vector Laboratories). The sections were counterstained by hematoxylin. For double immunofluorescent staining of samples, fluorescent secondary antibodies were applied to sections; DAPI was used in counter staining. Pictures were recorded using a Nikon Eclipse 80i fluorescence microscope (Melville, NY).

Real-time RT-PCR

Total RNAs from control vein or from AVF were isolated using the RNeasy kit (Qiagen, Valencia, CA). Real-time RT-PCR was performed using Opticon real-time RT-PCR machine (MJ Research, Waltham, MA). The specificity of real-time RT-PCR was confirmed using agarose gel electrophoresis and melting-curve analysis.

Western Blot Analysis

SMCs were lysed in RIPA buffer and ~20 μg of proteins were separated by SDS-PAGE. After transferring to NC membranes, antibodies were added.[54]

Statistical analysis

All data are presented as mean ± SE. Results were analyzed using Student's *t* test when results from 2 groups were compared or using two-way ANOVA when data from over 3 groups were studied; $p < 0.05$ was considered statistically significant.

Supplementary Material

Refer to Web version on PubMed Central for supplementary material.

Acknowledgments

We thank Dr. Begona Campos for preparation of human PTFE graft samples. This study was supported by grants from NIH RO1-DK095867, R37-DK37175, a grant from the American Heart Association (10SDG2780009), and a generous grant from Dr. and Mrs. Harold Selzman. We thank Dr. Yabin Chen for shipping the SMMHC-CreER^{T2} transgenic mice.

Abbreviation

AVF	arteriovenous fistula
CKD	chronic kidney disease

NICD	Notch intracellular domain
RBP-Jκ	recombination signal binding protein for immunoglobulin kappa J region
SMA-α	smooth muscle alpha actin
FSP-1	fibroblast specific protein 1

References

1. Roy-Chaudhury P, Sukhatme VP, Cheung AK. Hemodialysis vascular access dysfunction: A cellular and molecular viewpoint. J Am Soc Nephrol. 2006; 17:1112–1127. [PubMed: 16565259]
2. Allon M, Robbin ML. Increasing arteriovenous fistulas in hemodialysis patients: Problems and solutions. Kidney Int. 2002; 62:1109–1124. [PubMed: 12234281]
3. Dember LM, Susztak K. Notch ties a knot on fistula maturation. J Am Soc Nephrol. 2014; 25:648–650. [PubMed: 24480826]
4. Caplice NM, Wang S, Tracz M, et al. Neoangiogenesis and the presence of progenitor cells in the venous limb of an arteriovenous fistula in the rat. Am J Physiol Renal Physiol. 2007; 293:F470–475. [PubMed: 17344190]
5. Tanaka K, Sata M, Natori T, et al. Circulating progenitor cells contribute to neointimal formation in nonirradiated chimeric mice. Faseb J. 2008; 22:428–436. [PubMed: 17848623]
6. Arciniegas E, Frid MG, Douglas IS, et al. Perspectives on endothelial-to-mesenchymal transition: Potential contribution to vascular remodeling in chronic pulmonary hypertension. Am J Physiol Lung Cell Mol Physiol. 2007; 293:L1–8. [PubMed: 17384082]
7. Bentzon JF, Weile C, Sondergaard CS, et al. Smooth muscle cells in atherosclerosis originate from the local vessel wall and not circulating progenitor cells in apoe knockout mice. Arterioscler Thromb Vasc Biol. 2006; 26:2696–2702. [PubMed: 17008593]
8. Hoofnagle MH, Thomas JA, Wamhoff BR, et al. Origin of neointimal smooth muscle: We've come full circle. Arterioscler Thromb Vasc Biol. 2006; 26:2579–2581. [PubMed: 17110606]
9. Hu Y, Zhang Z, Torsney E, et al. Abundant progenitor cells in the adventitia contribute to atherosclerosis of vein grafts in apoe-deficient mice. The Journal of Clinical Investigation. 2004; 113:1258–1265. [PubMed: 15124016]
10. Shi Y, O'Brien JE Jr, Mannion JD, et al. Remodeling of autologous saphenous vein grafts. The role of perivascular myofibroblasts. Circulation. 1997; 95:2684–2693. [PubMed: 9193438]
11. Jiang X, Rowitch DH, Soriano P, et al. Fate of the mammalian cardiac neural crest. Development. 2000; 127:1607–1616. [PubMed: 10725237]
12. Echelard Y, Vassileva G, McMahon AP. Cis-acting regulatory sequences governing wnt-1 expression in the developing mouse cns. Development. 1994; 120:2213–2224. [PubMed: 7925022]
13. Hutson MR, Kirby ML. Model systems for the study of heart development and disease. Cardiac neural crest and conotruncal malformations. Semin Cell Dev Biol. 2007; 18:101–110. [PubMed: 17224285]
14. Waldo KL, Kumiski D, Kirby ML. Cardiac neural crest is essential for the persistence rather than the formation of an arch artery. Dev Dyn. 1996; 205:281–292. [PubMed: 8850564]
15. Kokubo T, Ishikawa N, Uchida H, et al. Ckd accelerates development of neointimal hyperplasia in arteriovenous fistulas. J Am Soc Nephrol. 2009; 20:1236–1245. [PubMed: 19423694]
16. Liang A, Wang Y, Han G, et al. Chronic kidney disease accelerates endothelial barrier dysfunction in a mouse model of an arteriovenous fistula. Am J Physiol Renal Physiol. 2013; 304:F1413–F1420. [PubMed: 23576636]
17. Spiekerkoetter E, Guignabert C, de Jesus Perez V, et al. S100a4 and bone morphogenetic protein-2 codependently induce vascular smooth muscle cell migration via phospho-extracellular signal-regulated kinase and chloride intracellular channel 4. Circ Res. 2009; 105:639–647. [PubMed: 19713532]

18. Cheng J, Wang Y, Liang A, et al. Fsp-1 silencing in bone marrow cells suppresses neointima formation in vein graft. Circ Res. 2012; 110:230–240. [PubMed: 22116816]
19. Wang Y, Liang A, Luo J, et al. Blocking notch in endothelial cells prevents arteriovenous fistula failure despite ckd. J Am Soc Nephrol. 2014; 25:773–783. [PubMed: 24480830]
20. Li Y, Takeshita K, Liu P-Y, et al. Smooth muscle notch1 mediates neointimal formation after vascular injury. Circ Res. 2009; 119:2686–2692.
21. Sakata Y, Xiang F, Chen Z, et al. Transcription factor chf1/hey2 regulates neointimal formation in vivo and vascular smooth muscle proliferation and migration in vitro. Athro Throm Vascul Biol. 2004; 24:2069–2074.
22. Tang Y, Urs S, Boucher J, et al. Notch and transforming growth factor-beta (tgfbeta) signaling pathways cooperatively regulate vascular smooth muscle cell differentiation. J Biol Chem. 2010; 285:17556–17563. [PubMed: 20368328]
23. Valdez Joseph M, Zhang L, Su Q, et al. Notch and tgfb1 form a reciprocal positive regulatory loop that suppresses murine prostate basal stem/progenitor cell activity. Cell Stem Cell. 2012; 11:676–688. [PubMed: 23122291]
24. Roy-Chaudhury P, Wang Y, Krishnamoorthy M, et al. Cellular phenotypes in human stenotic lesions from haemodialysis vascular access. Nephrol Dial Transplant. 2009; 24:2786–2791. [PubMed: 19377054]
25. Dember LM. Fistulas first-but can they last? Clinic J Am Soc Nephrol. 2011; 6:463–464.
26. Roy-Chaudhury P, Arend L, Zhang J, et al. Neointimal hyperplasia in early arteriovenous fistula failure. Am J Kidney Dis. 2007; 50:782–790. [PubMed: 17954291]
27. Hagensen MK, Shim J, Falk E, et al. Flanking recipient vasculature, not circulating progenitor cells, contributes to endothelium and smooth muscle in murine allograft vasculopathy. Arterioscler Thromb Vasc Biol. 2011; 31:808–813. [PubMed: 21233450]
28. Tanaka K, Sata M, Hirata Y, et al. Diverse contribution of bone marrow cells to neointimal hyperplasia after mechanical vascular injuries. Circ Res. 2003; 93:783–790. [PubMed: 14500338]
29. Daniel J-M, Bielenberg W, Stieger P, et al. Time-course analysis on the differentiation of bone marrow-derived progenitor cells into smooth muscle cells during neointima formation. Arthro Throm Vascul Biol. 2010; 30:1890–1896.
30. Diao Y, Guthrie S, Xia SL, et al. Long-term engraftment of bone marrow-derived cells in the intimal hyperplasia lesion of autologous vein grafts. Am J Pathol. 2008; 172:839–848. [PubMed: 18276778]
31. Skartsis N, Manning E, Wei Y, et al. Origin of neointimal cells in arteriovenous fistulae: Bone marrow, artery, or the vein itself? Semin Dial. 2011; 24:242–248. [PubMed: 21517994]
32. Yang B, Janardhanan R, Vohra P, et al. Adventitial transduction of lentivirus-shrna-vegf-a in arteriovenous fistula reduces venous stenosis formation. Kidney Int. 2014; 85:289–306. [PubMed: 23924957]
33. Shi Y, O'Brien JE, Fard A, et al. Adventitial myofibroblasts contribute to neointimal formation in injured porcine coronary arteries. Circulation. 1996; 94:1655–1664. [PubMed: 8840858]
34. Forbes MS, Thornhill BA, Chevalier RL. Proximal tubular injury and rapid formation of atubular glomeruli in mice with unilateral ureteral obstruction: A new look at an old model. Am J Physiol Renal Physiol. 2011; 301:F110–117. [PubMed: 21429968]
35. Ivaska J, Pallari HM, Nevo J, et al. Novel functions of vimentin in cell adhesion, migration, and signaling. Exp Cell Res. 2007; 313:2050–2062. [PubMed: 17512929]
36. Kreis S, Schonfeld HJ, Melchior C, et al. The intermediate filament protein vimentin binds specifically to a recombinant integrin alpha2/beta1 cytoplasmic tail complex and co-localizes with native alpha2/beta1 in endothelial cell focal adhesions. Exp Cell Res. 2005; 305:110–121. [PubMed: 15777792]
37. Dave JM, Bayless KJ. Vimentin as an integral regulator of cell adhesion and endothelial sprouting. Microcirculation. 2014; 21:333–344. [PubMed: 24387004]
38. Nieminen M, Henttinen T, Merinen M, et al. Vimentin function in lymphocyte adhesion and transcellular migration. Nat Cell Biol. 2006; 8:156–162. [PubMed: 16429129]
39. Cai WJ, Koltai S, Kocsis E, et al. Remodeling of the adventitia during coronary arteriogenesis. Am J Physiol Heart Circ Physiol. 2003; 284:H31–40. [PubMed: 12388238]

40. Li ZH, Bresnick AR. The s100a4 metastasis factor regulates cellular motility via a direct interaction with myosin-iia. Cancer Res. 2006; 66:5173–5180. [PubMed: 16707441]
41. Yammani RR, Carlson CS, Bresnick AR, et al. Increase in production of matrix metalloproteinase 13 by human articular chondrocytes due to stimulation with s100a4: Role of the receptor for advanced glycation end products. Arthritis Rheum. 2006; 54:2901–2911. [PubMed: 16948116]
42. Bjornland K, Winberg JO, Odegaard OT, et al. S100a4 involvement in metastasis: Deregulation of matrix metalloproteinases and tissue inhibitors of matrix metalloproteinases in osteosarcoma cells transfected with an anti-s100a4 ribozyme. Cancer Res. 1999; 59:4702–4708. [PubMed: 10493528]
43. Brisset AC, Hao H, Camenzind E, et al. Intimal smooth muscle cells of porcine and human coronary artery express s100a4, a marker of the rhomboid phenotype in vitro. Circ Res. 2007; 100:1055–1062. [PubMed: 17347479]
44. Caolo V, Schulten HM, Zhuang ZW, et al. Soluble jagged-1 inhibits neointima formation by attenuating notch-herp2 signaling. Arterioscler Thromb Vasc Biol. 2011; 31:1059–1065. [PubMed: 21330605]
45. Chen M, Sinha M, Luxon BA, et al. Integrin alpha6beta4 controls the expression of genes associated with cell motility, invasion, and metastasis, including s100a4/metastasin. J Biol Chem. 2009; 284:1484–1494. [PubMed: 19011242]
46. Chen M, Sastry SK, O'Connor KL. Src kinase pathway is involved in nfat5-mediated s100a4 induction by hyperosmotic stress in colon cancer cells. Am J Physiol Cell Physiol. 2011; 300:C1155–1163. [PubMed: 21289293]
47. Lawrie A, Spiekerkoetter E, Martinez EC, et al. Interdependent serotonin transporter and receptor pathways regulate s100a4/mts1, a gene associated with pulmonary vascular disease. 2005; 97:227–235.
48. Wong CY, de Vries MR, Wang Y, et al. Vascular remodeling and intimal hyperplasia in a novel murine model of arteriovenous fistula failure. J Vasc Surg. 2014; 59:192–201. e191. [PubMed: 23684425]
49. Zhang L, Wang XH, Wang H, et al. Satellite cell dysfunction and impaired igf-1 signaling cause ckd-induced muscle atrophy. J Am Soc Nephrol. 2010; 21:419–427. [PubMed: 20056750]
50. Zhang L, Rajan V, Lin E, et al. Pharmacological inhibition of myostatin suppresses systemic inflammation and muscle atrophy in mice with chronic kidney disease. FASEB J. 2011; 25:1653–1663. [PubMed: 21282204]
51. Cheng J, Truong LD, Wu X, et al. Serum- and glucocorticoid-regulated kinase 1 is upregulated following unilateral ureteral obstruction causing epithelial-mesenchymal transition. Kidney Int. 2010; 78:668–678. [PubMed: 20631674]
52. Wu X, Cheng J, Li P, et al. Mechano-sensitive transcriptional factor egr-1 regulates insulin-like growth factor-1 receptor expression and contributes to neointima formation in vein grafts. Arterioscler Thromb Vasc Biol. 2009 ATVBAHA.109.184259.
53. Ranjzad P, Salem HK, Kingston PA. Adenovirus-mediated gene transfer of fibromodulin inhibits neointimal hyperplasia in an organ culture model of human saphenous vein graft disease. Gene Ther. 2009; 16:1154–1162. [PubMed: 19474808]
54. Cheng J, Wang Y, Ma Y, et al. The mechanical stress-activated serum-, glucocorticoid-regulated kinase 1 contributes to neointima formation in vein grafts. Circ Res. 2010; 107:1265–1274. [PubMed: 20884880]

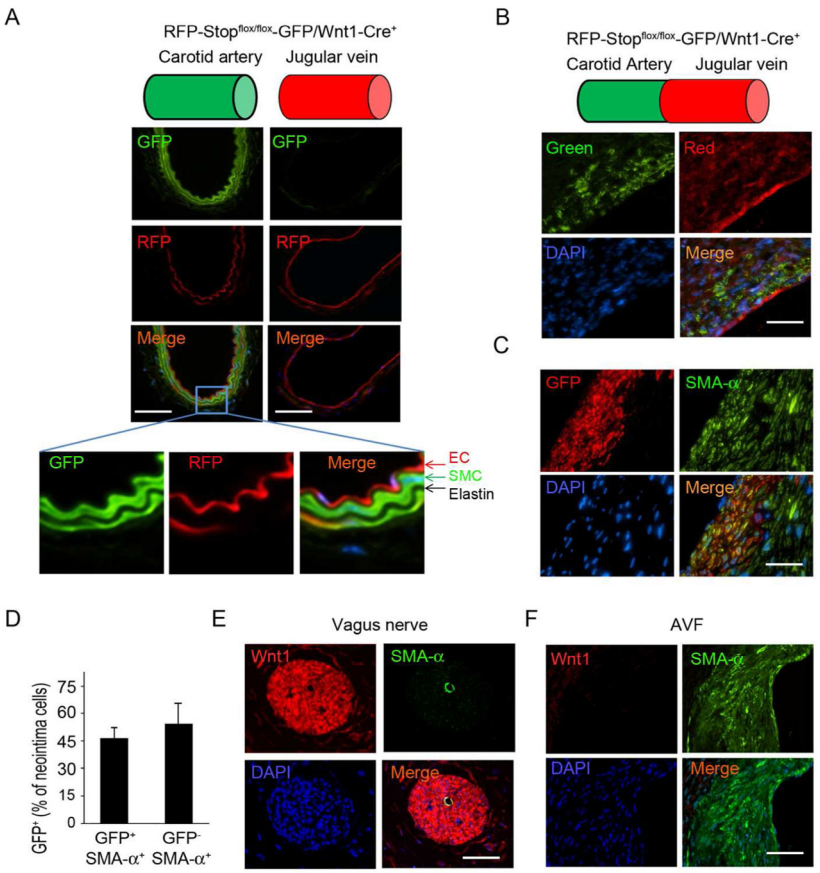

Figure 1.

SMCs from the anastomosed artery contribute to neointima formation in AVFs. A. Wnt1-Cre-mediated GFP expression in SMCs of the common carotid artery in RFP-Stop$^{flox/flox}$-GFP/Wnt1-Cre^{+} mice. Frozen sections of arteries or jugular veins were assessed by fluorescent microscopy (EC, endothelial cell). B. AVFs were created in RFP-Stop$^{flox/flox}$-GFP/Wnt1-Cre^{+} mice and the frozen sections were prepared to detect fluorescent signals without immunostaining. The positive signals were recorded under green and red channels. C. AVFs were created in RFP-Stop$^{flox/flox}$-GFP/Wnt1-Cre^{+} mice and collected in paraffin section (this treatment eliminated fluorescent signals), and GFP-positive cells incorporated into the neointima were detected using immunostaining with anti-GFP (red) or SMA-α-FITC antibodies (green). D. Statistical analysis of GFP positive cells in total of SMA-α positive neointima cells. Total 5 slides from each AVF sample were counted under 400 X view (n = 4). E & F. Wnt1 expression was examined by immunofluorescent staining in vagus nerve (E) and in AVFs (F). (Scale: 50 μm; n = 4).

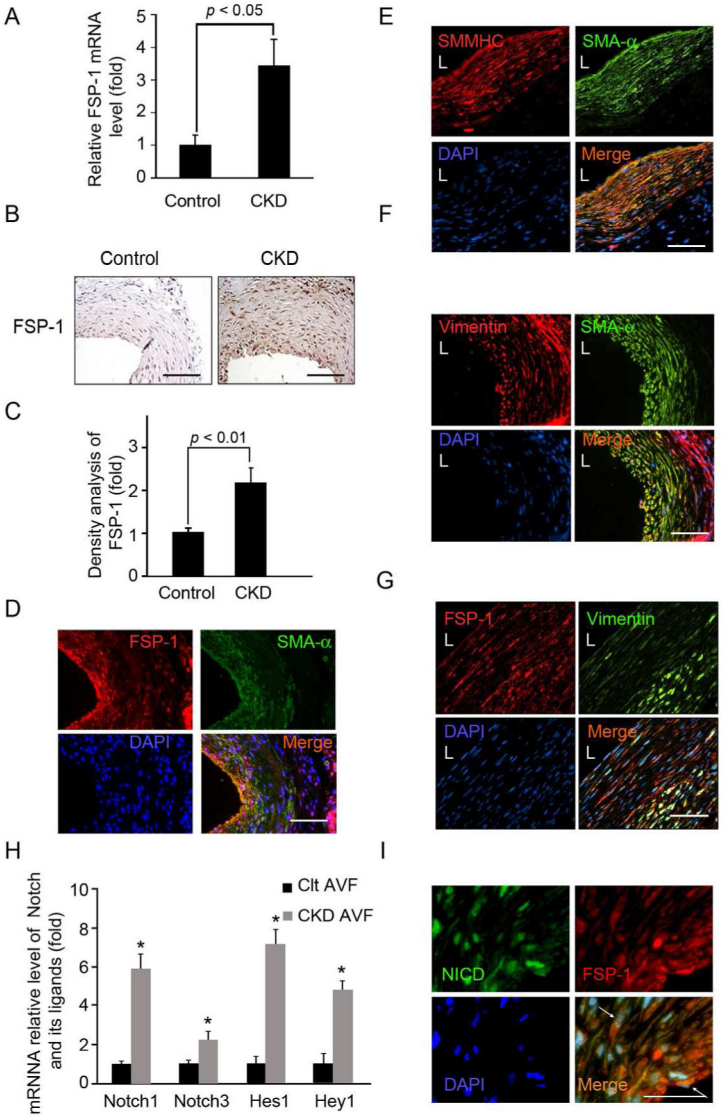

Figure 2.

In mice with CKD, FSP-1 and activated Notch1 are expressed in AVFs. A. FSP-1 mRNA was detected (RT-PCR) was 3.5-fold greater in AVFs of CKD mice vs. control. B. Expression of FSP-1 was detected by immunohistochemistry (n = 4 per group). C. Density analysis of FSP-1 levels from panel B. D & E. Co-immunostaining of SMA-α with FSP-1 (D) or SMC terminal differentiation marker SMMHC (E) in AVFs. F & G. Vimentin was co-immunostained with SMA-α (F) and FSP-1 (G) in AVFs. H. AVFs were prepared from control and CKD mice, Notch receptor and their target genes were detected by real time RT-PCR (*, $p < 0.05$). I. In AVFs from CKD mice, SMCs expressing N1ICD co-stained positively for FSP-1. The expression of N1ICD (green) and FSP-1 (red) were determined by double immunostaining (See arrows). Scale: 50 μm; L, lumen.

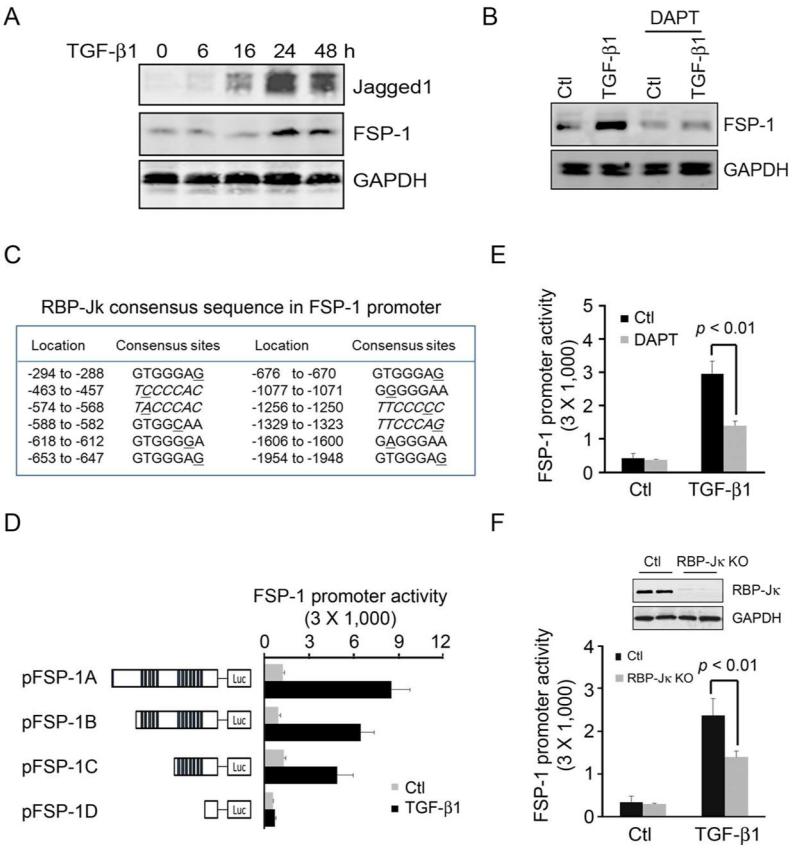

Figure 3.

RBP-Jκ regulates TGF-β1-induced FSP-1 expression. A. TGF-β1 stimulates Jagged1 and FSP-1 expression in a time-dependent fashion in SMCs. B. TGF-β1-induced FSP-1 expression was mediated by Notch. SMCs were pretreated with Notch inhibitor, DAPT, and then exposed to TGF-β1 for 24 h; FSP-1 was detected by Western blot. C. Potential RBP-Jκ binding sites in the mouse FSP-1 promoter are identified, and mismatched bases are underlined. D. FSP-1 promoter fragments were cloned into a luciferase vector and RBP-Jκ potential binding sites are marked with bars. The luciferase plasmids were cotranfected into SMCs with pTK-Renilla luciferase plasmid. At 24 h after TGF-β1 or solvent addition, luciferase activities were detected. E. SMCs were transfected with the FSP-1 promoter plasmid (pFSP-1A), and then pretreated with or without DAPT for 2 h, followed by treatment with TGF-β1. Luciferase activity was detected after 24 h (mean ± SE; 3 repeated experiments). F. SMCs were isolated from RBP-Jκ$^{flox/flox}$ mice and treated with Ad-Cre to KO RBP-Jκ. (Ad-vector infected cells were the control). SMCs from control and RBP-Jκ KO mice were transfected with the FSP-1 promoter plasmid in the presence or absence of TGF-β1; luciferase activity was detected after 24 h (mean ± SE, 3 repeated experiments).

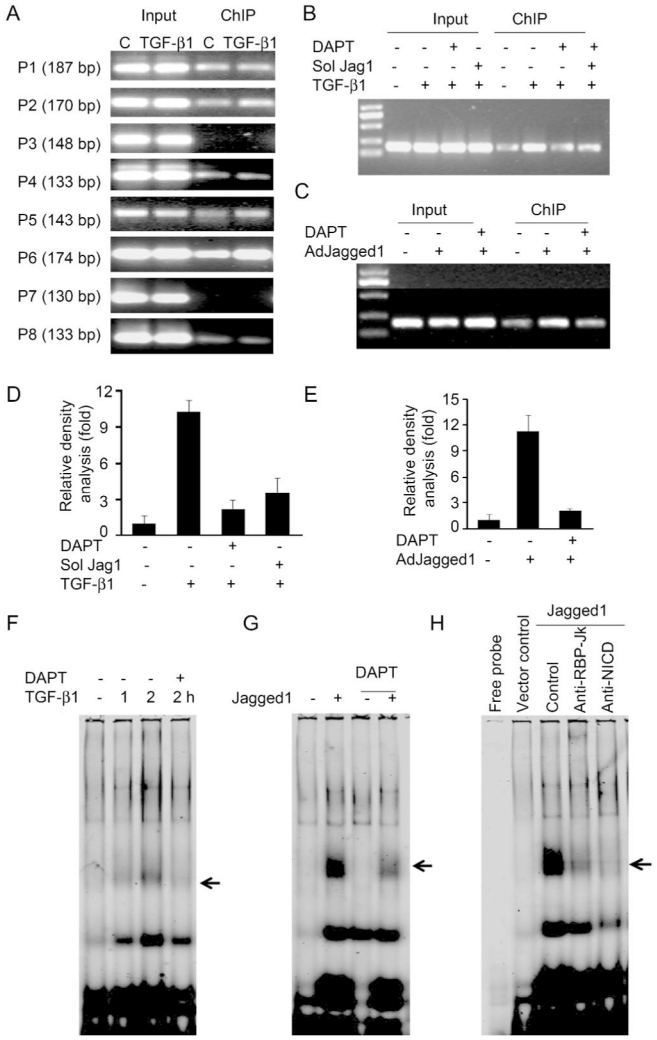

Figure 4.

Notch mediates DNA binding activity in FSP-1 promoter. A. ChIP analysis of TGF-β1-induced DNA binding activity to the FSP-1 promoter of SMCs was evaluated by immunoprecipitation with N1ICD antibodies followed by PCR to detect the DNA binding activity. Representative data from 3 repeated experiments are shown. B. TGF-β1-induced DNA binding activity was inhibited by Notch inhibitors. SMCs pretreated with DAPT or infected with soluble Jagged1 before SMCs were treated with TGF-β1 for 2 h; DNA binding activity was detected by ChIP assay. C. SMCs infected with AdJagged1 (full length) in the presence/absence of Notch inhibitors, DAPT or soluble Jagged1 were used in ChIP assays. D & E. Relative density analysis of results from Panel B & C, respectively. F. Electrophoretic mobility shift assay (EMSA) of Notch-dependent binding activity induced in the FSP-1 promoter by TGF-β1 treatment. SMCs were examined with or without 30 min of pretreatment with 10 μM DAPT followed by 2h of TGF-â1 treatment. Nuclear proteins were incubated with the Dye-680 labeled probe (P6). G. SMCs infected with the Jagged1 adenovirus or vector for 24 h were examined by EMSA in 3 repeated experiments. H. A super-shift analysis of Jagged1-induced DNA binding activity to the FSP-1 promoter: SMCs

were treated with vector or AdJagged1. Nuclear proteins from SMCs were incubated with the indicated antibodies for 1 h before the EMSA analysis was undertaken.

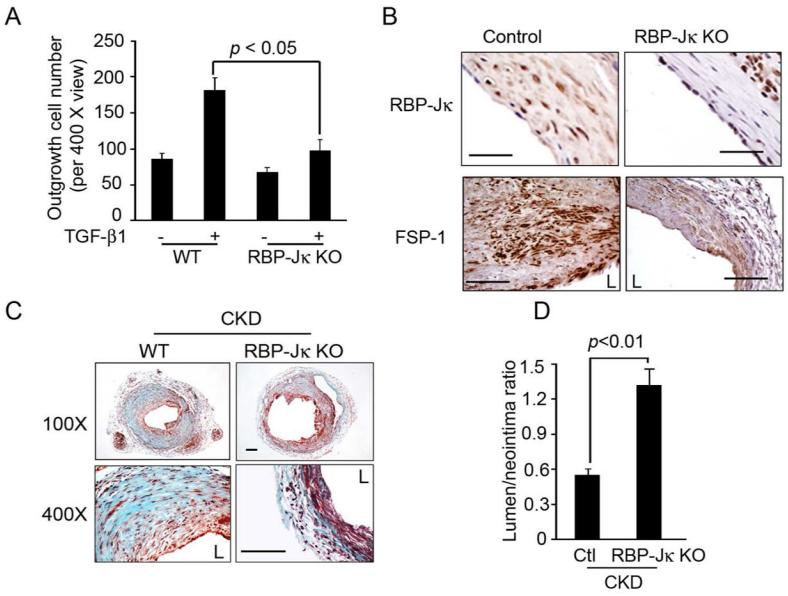

Figure 5.

Notch regulates SMC migration and neointima formation in AVFs. A. TGF-β1 regulated out-growth of SMCs was Notch-dependent: artery fragments from WT and RBP-Jκ KO mice were seeded into DMEM media-filled plates. TGF-β1 was added, after 7 days, outgrowing SMCs were counted (Representative data from 3 animals). B. Inducible KO of RBP-Jκ in SMCs of AVFs. AVFs from RBP-$J\kappa^{flox/flox}$/SMMHC-$CreER2^{+}$ mice were treated with or without tamoxifen, RBP-Jκ and FSP-1 expression in AVFs were detected by immunostaining. Tamoxifen-treated mice had virtually no RBP-Jκ expression in neointima cells. C. Trichrome staining of of AVFs created in Control and RBP-Jκ KO mice with CKD is shown. D. RBP-Jκ KO inhibits FSP-1 expression as detected by immunostaining in AVFs created in Control and RBP-Jκ KO mice with CKD. F. The ratio of lumen to neointima areas was improved in RBP-Jκ KO mice. (L, lumen). Scale: 50 μm.

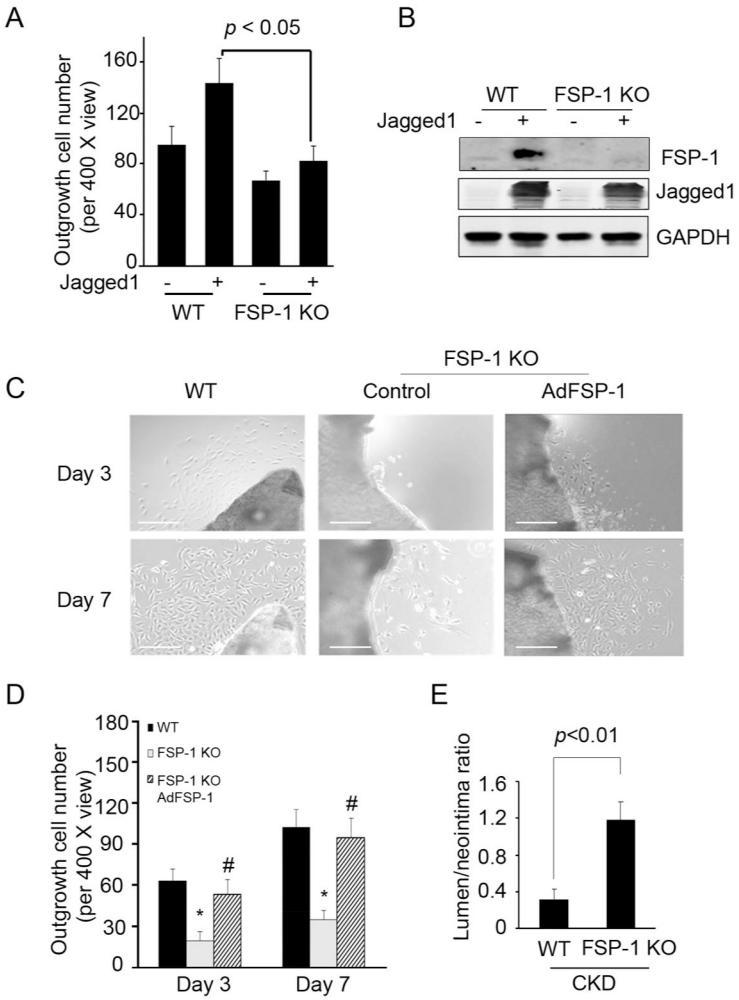

Figure 6.

FSP-1 KO suppresses SMC migration and CKD-induced neointima formation. A. Common carotid arteries from WT or FSP-1 KO mice were cut into small pieces and cultured in DMEM. Pieces of arteries from WT or FSP-1 KO mice were infected with full length AdJagged1 or control adenovirus on day 2. SMC outgrowth was determined after 7 days. Representative data from two repeated experiments are shown. B. Jagged1 expression induced FSP-1 expression. SMCs from WT or FSP-1 KO mice were infected with a Jagged1 adenovirus and FSP1 was detected. C. FSP-1 KO inhibits SMC outgrowth. Pieces of common carotid arteries from WT or FSP-1 KO mice were cultured in DMEM. They were infected with AdFSP-1 or control adenovirus on day 2. SMC outgrowth was determined after 3 and 7 days (Scale: 50 μm). D. The number of outgrowing cells in a total of 3 views from 3 samples in each group was counted. E. In mice with CKD, the ratio of the lumen to neointima areas in AVFs from FSP-1 KO mice were compared to values from WT mice (mean ± SE, n = 5).

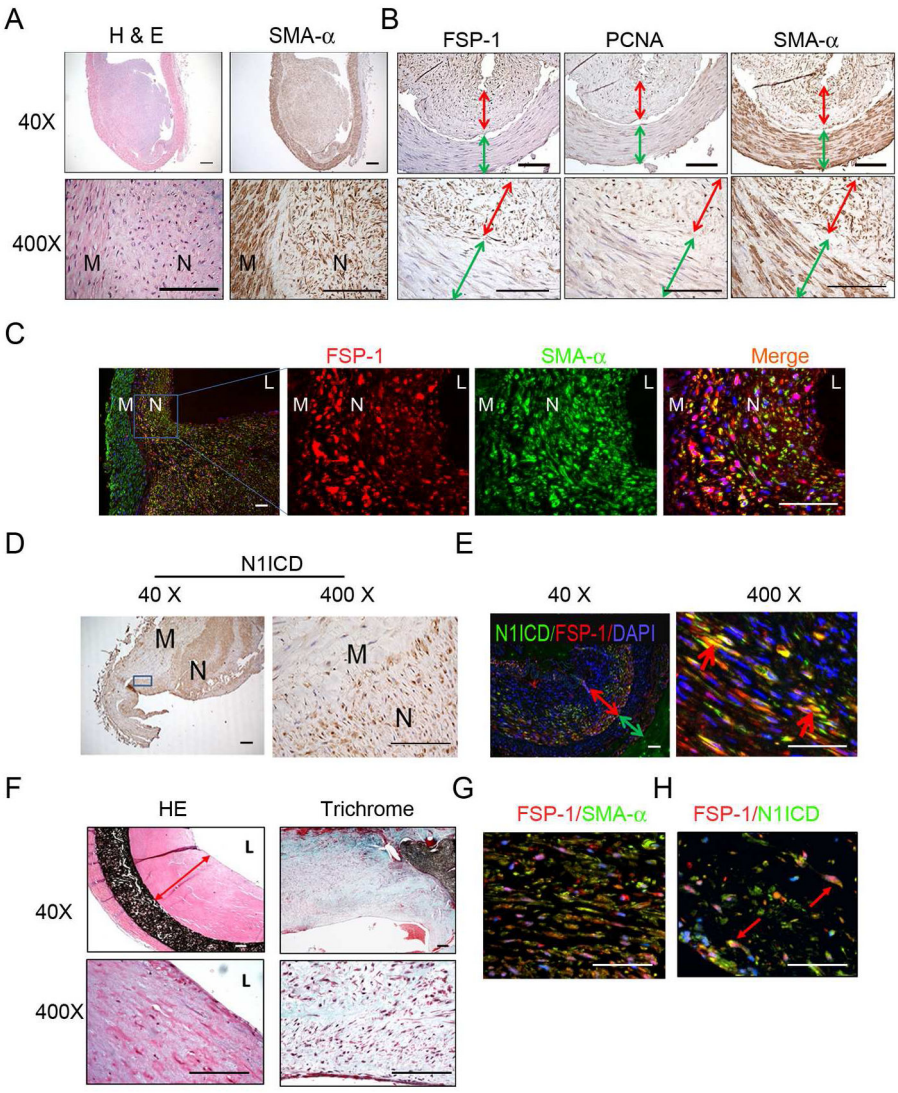

Figure 7.

In failed AVFs from ESRD patients, FSP-1 is expressed in neointima cells. A. Morphology and SMA-α-positive cells from failed AVFs of ESRD patients (n =5). H & E (left panel) and SMA-α immunostaining (right panel) are shown. B. Characterization of neointima cells found in AVFs from ESRD patients. Cross sections of AVFs were immunostained for the FSP-1, PCNA, and SMA-α. (Red, double headed arrows show the neointima thickness, and green arrows indicate the media of AVFs). C. Coimmunostaining of FSP-1 and SMA-α in AVFs revealed that FSP-1 positive cells also express SMA-α. D. Activated Notch (N1ICD, brown color) is mainly located in nuclei of neointima cells in the failed AVFs of ESRD patients. E. In AVFs from ESRD patients, SMCs expressing N1ICD co-stained positively for FSP-1. The expression of N1ICD (green) and FSP-1 (red) were determined by double immunostaining; the double-head arrow indicates the neointima (red) and the smooth muscle layer of the vein (green). The red arrow points to cells stained positively for N1ICD and FSP-1. (N, neointima; M, media; L, lumen). Scale: 50 μm. F. Staining for H & E (Left panel) and Masson Trichome (Right panel) of human PTFE grafts are shown. Representative

pictures from two PTFE grafts are shown. G. Co-immunofluorescent of SMA-α and FSP-1 in PTFE graft revealed that FSP-1 positive cells also express SMA-α. H. In PTFE graft from ESRD patients, expression of N1ICD and FSP-1 was detected by immunofluorescent staining with FSP-1 (n = 7).